European Journal of Pharmaceutical Sciences 189 (2023) 106524

Contents lists available at ScienceDirect

European Journal of Pharmaceutical Sciences

journal homepage: www.elsevier.com/locate/ejps

Exploring the use of modified *in vitro* digestion assays for the evaluation of ritonavir loaded solid lipid-based formulations

Ioannis I. Andreadis [a,b], Arne Schulzen [c], Julian Quodbach [d], Christel A.S. Bergström [a,e,*]

[a] Department of Pharmacy, Uppsala University, P.O. Box 580, SE-751 23, Uppsala, Sweden
[b] Laboratory of Pharmaceutical Technology, Department of Pharmacy, Faculty of Health Sciences, Aristotle University of Thessaloniki, GR-54124, Thessaloniki, Greece
[c] Institute of Pharmaceutics and Biopharmaceutics, Heinrich Heine University, Universitätsstraße 1, DE-40225, Düsseldorf, Germany
[d] Department of Pharmaceutics, Utrecht University, Universiteitsweg 99, 3584 CG, Utrecht, the Netherlands
[e] The Swedish Drug Delivery Center, Department of Pharmacy, Uppsala University, P.O. Box 580, SE-751 23, Uppsala, Sweden

ARTICLE INFO

Keywords:
In vitro model
Lipid digestion
Solid lipid based formulation
Ritonavir
Oral drug delivery

ABSTRACT

Solid lipid-based formulations (sLBFs) have the potential to increase the oral bioavailability of drugs with poor solubility in water, while counteracting some of the disadvantages of liquid LBFs. The most common experimental set-up to study the performance of LBFs *in vitro* is the lipolysis assay, during which the LBFs are digested by lipases in an environment mimicking the human small intestine. However, this assay has failed in many cases to correctly predict the performance of LBFs *in vivo*, highlighting the need for new and improved *in vitro* assays to evaluate LBFs at the preclinical stage. In this study, the suitability of three different *in vitro* digestion assays for the evaluation of sLBFs was assessed; the classic one-step intestinal digestion assay, a two-step gastrointestinal digestion assay and a bicompartmental assay permitting the simultaneous monitoring of digestion and permeation of the active pharmaceutical ingredient (API) across an artificial membrane (Lecithin in Dodecane – LiDo). Three sLBFs (M1-M3) with varied composition and ritonavir as model drug were prepared and examined. When comparing the ability of these formulations to keep the drug solubilized in the aqueous phase, all three assays show that M1 performs better, while M3 presents poor performance. However, the classic *in vitro* intestinal digestion assay fails to provide a clear ranking of the three formulations, something that is more evident when using the two modified and more physiologically relevant assays. Also, the two modified assays provide additional information about the performance of the formulations including the performance in the gastric environment and intestinal flux of the drug. These modified *in vitro* digestion assays are valuable tools for the development and evaluation of sLBFs to make better informed decisions of which formulations to pursue for *in vivo* studies.

1. Introduction

Oral drug administration is usually perceived as the most advantageous route for drug delivery. (Carrière, 2016) Formulating poorly water-soluble active pharmaceutical ingredients (APIs) for *per os* administration remains a major challenge for the pharmaceutical industry, (Fernandez et al., 2009) as the majority of new drug molecules developed belong to this category. (Carrière, 2016; Fernandez et al., 2013) The poor oral bioavailability of lipophilic drugs could potentially be improved when formulated in lipid-based formulations (LBFs) due to the increased apparent solubility and permeability and decreased drug metabolism before the drug reaches the systemic circulation. (Carrière,

Abbreviations: 4-BBBA, 4-bromophenylboronic acid; ACN, Acetonitrile; AIDS, Acquired Immunodeficiency Syndrome; API, Active pharmaceutical ingredient; ANOVA, Analysis of variance; AUC, Area under the curve; BCS, Biopharmaceutics Classification System; DSC, Differential scanning calorimetry; DMSO, Dimethylsulfoxide; TPGS, D-α-tocopherol polyethylene glycol 1000 succinate; ENA, Enabling Absorption; FaSSIF, Fasted State Simulated Intestinal Fluid; FeSSIF, Fed State Simulated Intestinal Fluid; FaSSGF, Fasted State Stimulated Gastric Fluid; FFAs, Free fatty acids; HPLC, High pressure liquid chromatography; HLB, Hydrophilic lipophilic balance; IVIVC, In vitro-in vivo correlation; LiDo, Lecithin in Dodecane; LBF, Lipid based formulation; LY, Lucifer Yellow; PBS, Phosphate Buffered Saline; PEG, Polyethylene glycol; PVDF, Polyvinylidene fluoride; PVPA, Poly(vinylphosphonic acid); sLBF, Solid Lipid-Based Formulation; UV, Ultraviolet; XRD, X-Ray Diffraction.

* Corresponding author at: Department of Pharmacy, Uppsala University, P.O. Box 580, SE-751 23, Uppsala, Sweden.
E-mail address: christel.bergstrom@farmaci.uu.se (C.A.S. Bergström).

https://doi.org/10.1016/j.ejps.2023.106524
Received 11 April 2023; Received in revised form 25 June 2023; Accepted 9 July 2023
Available online 9 July 2023

2016; Keemink et al., 2022; Silva et al., 2018) The use of LBFs may also reduce food effects on drug absorption. (Hedge and Bergström, 2020) Nevertheless, the increased oral bioavailability seems to be a result of the interactions of the LBF components and their metabolites with biliary amphiphilic molecules and other lipids physiologically present in the digestive system. (Fernandez et al., 2013)

LBFs usually consist of lipids, or mixtures of lipids with surfactants and cosolvents (Carrière, 2016; Feeney et al., 2016; Klitgaard et al., 2020) and are formulated as liquid-filled soft gelatin capsules. (Silva et al., 2018) The plethora of disadvantages of these dosage forms are associated with interactions of excipients with the capsule shell, leakage, inconvenient handling, instability and possible API precipitation, and has triggered interest in solidified LBFs (sLBFs). (Silva et al., 2018; Vithani et al., 2017) These sLBFs could potentially overcome some of these drawbacks, as they show improved stability, dosing accuracy, patient compliance and safety, while keeping costs low. (Silva et al., 2018) An abundance of techniques have been employed for their production including the use of solid carriers as absorptive materials, melt extrusion and granulation and spray drying among others. (Silva et al., 2018; Vithani et al., 2017; Vithani et al., 2019) To successfully formulate sLBFs with these methods, solid-phase carriers (*e.g.*, silica, magnesium aluminometasilicate, cellulose, etc.) are needed in large amounts, something that can potentially cause additional problems, like dose dilution, toxicity issues and incomplete drug release. (Vithani et al., 2019; Van Speybroeck et al., 2012; Williams et al., 2014) Alternatively, sLBFs can also be formulated as solid or semi solid dosage forms when lipids with high melting points are used. (Feeney et al., 2016)

Most lipids contain ester bonds and are highly affected by the presence of lipases, which leads to the formation of monoglycerides and free fatty acids. (Vithani et al., 2017) Physiologically, lipid digestion begins in the stomach, where the ester bonds of the triglycerides are cleaved by the gastric lipase, and continues in the small intestine, where the pancreatic lipase—secreted by the pancreas along with colipase—takes over. (Fernandez et al., 2009) Even though gastric lipid digestion is only accountable for 10% to 25% of the total lipolysis, the metabolites generated through this phase affect the activation of the secretive function of the bile and the pancreas. (Fernandez et al., 2013) Furthermore, the products of the digestion of the lipid components of the LBFs play a key role in the dispersion, solubilization and absorption of the drug. (Carrière, 2016; Fernandez et al., 2013) Digestion products interact with biomolecules present in the gastrointestinal tract and jointly they assemble into colloidal structures capable of solubilizing and transporting lipophilic drugs. (Vithani et al., 2019)

The most commonly used *in vitro* tool to estimate the *in vivo* performance of LBFs is the *in vitro* digestion assay, (Tanaka et al., 2021) during which LBFs are dispersed in a biorelevant intestinal medium where they are later digested by pancreatic lipases. (Hedge and Bergström, 2020) The assay enables quantification of the digestibility of the lipids by making use of titration of the released free fatty acids with NaOH. At the same time the drug concentration in the aqueous phase, *i.e.*, the amount of drug that is available for absorption, is measured via sampling of the medium followed by separation of the different phases formed during digestion through centrifugation. (Keemink et al., 2022; Keemink et al., 2019) However, this assay often fails to provide adequate *in vitro-in vivo* correlation (IVIVC), (Keemink et al., 2022; Hedge and Bergström, 2020) suggesting that increased solubility and supersaturation in the luminal compartment (here mimicked with enzyme-spiked biorelevant medium) cannot completely explain how LBFs affect drug bioavalability. (Hedge and Bergström, 2020) This also emphasizes the need for new or modified *in vitro* methods with improved predictive value for the oral bioavailability of drugs during preclinical studies (Klitgaard et al., 2020) to avoid costly, time-consuming and most importantly unnecessary *in vivo* animal studies. (Keemink et al., 2022; Sams et al., 2016) To date, the standard digestion model can rather be viewed as a product performance testing similarly to dissolution studies, without necessarily providing information about absorption to the systemic circulation.

In vitro digestion assays are usually performed in a single step representing the physiology of the upper small intestine, disregarding the digestion of lipids happening during the passage of the LBF from the stomach. (Fernandez et al., 2013; Chatzidaki et al., 2016) The gastric pH can possibly affect the intestinal absorption and the overall bioavailability of weak bases (Christophersen et al., 2014) and the gastric lipase is known to influence the lipid digestion and pancreatic lipase activity. (Chatzidaki et al., 2016) Thus, the addition of a gastric phase in the *in vitro* digestion experiments has been suggested as a means to improve the predictive power of these *in vitro* assays. (Christophersen et al., 2014) Various protocols have been suggested for an *in vitro* gastrointestinal lipolysis assay and they have been used to test the digestion of food components, (Chabni et al., 2022) excipients (Fernandez et al., 2013) and drug-loaded formulations. (Fernandez et al., 2009) Additionally, most *in vitro* digestion assays do not take into account the absorption of the drug. This means that the predicted *in vivo* performance of LBFs might be underestimated and drug precipitation might be overestimated, as the irrelevant high supersaturation level obtained during the assay may trigger precipitation of the drug. The presence of a physiologically relevant absorption compartment can potentially improve the prediction of *in vivo* performance, as it represents an alternative route for the drug towards a more thermodynamically stable sink environment. (Keemink et al., 2019) Keemink et al. developed a set-up that could capture both LBF digestion and drug permeation simultaneously and used it to successfully correlate *in vitro* with *in vivo* data. (Keemink et al., 2019)

In the present study, three different solid LBFs (sLBFs) were prepared using lipidic excipients with melting points higher than room temperature. Table 1 the model drug used in this study was ritonavir; a BCS (Biopharmaceutics Classification System) class IV antiretroviral agent with low water solubility and permeability widely used in the treatment of Acquired Immunodeficiency Syndrome (AIDS). (Rossi et al., 2007; Velozo et al., 2022) The developed sLBFs were tested *in vitro* using the classic intestinal digestion assay, a two-step gastrointestinal digestion assay and a lipolysis-permeability assay. The aim of this study was to investigate the suitability of these three different experimental setups for the *in vitro* testing of the sLBFs and to examine how the varying composition of the sLBFs affects their performance.

2. Materials and methods

2.1. Materials

Acetonitrile (ACN, ≥ 99.9%), dimethyl sulfoxide (DMSO, ≥ 99.9%), methanol (≥ 99.9%), pancreatin from porcine pancreas (8 x USP specifications), lipase from *Rhizopus oryzae* (≥ 30 U/mg), 4-bromophenylboronic acid (4-BBBA, ≥ 95.0%), D-α-tocopherol polyethylene glycol 1000 succinate (TPGS), Trizma® maleate (TRIS maleate salt), sodium hydroxide (NaOH) pellets, sodium chloride (NaCl), potassium chloride (KCl), calcium chloride ($CaCl_2$) granules, sodium phosphate monobasic

Table 1
Chemical description and melting range of excipients used in this study.

Excipient name	Chemical description	Melting range (°C)
WITEPSOL® E 85	Hard fat – Mono-, di-, and triglycerides (C12 – C18)	43
Gelucire® 48/16	PEG-32 esters of palmitic and stearic acid	46 - 50
IMWITOR® 491	Glyceryl monostearate	66 - 77
DYNASAN® 116	Glyceryl tripalmitate	63 - 68
Gelucire® 50/13	Mono-, di-, triglycerides and PEG-32 mono-, diesters of palmitic and stearic acid	46 - 51

dihydrate (NaH_2PO_4–$2H_2O$) and potassium phosphate monobasic (KH_2PO_4) were purchased from Merck (Darmstadt, Germany). WITEPSOL® E 85 pastilles, IMWITOR® 491 powder and DYNASAN® 116 flakes were kindly provided from IOI Oleo GmbH (Hamburg, Germany). Gelucire® 48/16 and Gelucire® 50/13 pellets were kindly donated by Gattefossé (Saint-Priest, France). Ethanol (99.5%, denatured with 100 g isopropyl alcohol) and n-dodecane (≥ 99%) were purchased from Solveco (Rosersberg, Sweden) and Alfa Aesar (Lancashire, UK), respectively. Lecithin (L-α-phosphatidylcholine) Soy PC extract (20%) was obtained from Avanti Polar Lipids (Alabaster, AL, USA). Ritonavir (> 99%) was purchased from Shanghai Desano Pharmaceuticals Co., Ltd. (Shanghai, China) and Lucifer yellow (LY) CH dilithium salt was purchased from Biotium (Fremont, CA, USA). FaSSIF/FeSSIF/FaSSGF powder was obtained from biorelevant.com (London, UK). Ultrapure Milli-Q® water (grade I) from a direct water purification system (Merck, Darmstadt, Germany) was used for all the experiments.

2.2. Preparation of buffers and media

The medium used for the intestinal lipolysis studies (Fasted State Simulated Intestinal Fluid – FaSSIF) consisted of a buffer of 150 mM NaCl, 2 mM TRIS maleate and 1.4 mM $CaCl_2$ supplemented with 2.24 g/L FaSSIF powder. The pH was adjusted to 6.5.

For the gastrointestinal lipolysis studies, the medium used (Fasted State Simulated Gastric Fluid – FaSSGF) contained 34.2 mM NaCl and 0.06 g/L FaSSGF powder and pH was adjusted to 2.5. Thirty minutes after the initiation of the gastric phase, a concentrated lipolysis medium consisting of 878.96 mM NaCl, 14.59 mM TRIS maleate, 10.21 mM $CaCl_2$ and 15.98 g/L FaSSIF powder was added to the vessel to achieve final concentrations and pH similar to those of the medium used for the intestinal lipolysis studies.

The medium used in the donor compartment for the lipolysis-permeation studies was the same as the one used for the lipolysis studies, but with a higher TRIS-maleate concentration (200 mM) in order to achieve a higher buffering capacity, as titration during the digestion was not possible (see paragraph 2.7.2.). The receiver compartment was filled with Phosphate Buffered Saline (PBS) (pH 7.4) (137 mM NaCl, 2.7 mM KCl, 10 mM Na_2HPO_4–$2H_2O$, 1.8 mM KH_2PO_4) with the addition of 0.2% w/v TPGS.

2.3. Solid lipid-based formulations

2.3.1. Preparation of the solid lipid-based formulations

Three sLBFs (M1-M3) with varying composition were prepared according to Table 2; all had a drug load of 10% w/w. Mixtures were accurately weighed and subsequently stirred with a magnetic stirrer (MR Hei Standard, Heidolph Instruments GmbH & Co., Schwabach, Germany) at 130 °C and 250 rpm for 15 min. The melted mixtures were left to cool down to room temperature under constant stirring. After solidification, the formulations were further cooled using liquid nitrogen and milled with a food processor (AICOK TB138M, Aicok Home Essentials). The milled formulations were sieved using a vibratory sieve shaker (AS 200 Control, Retsch GmbH, Haan, Germany) at 1.5 mm amplitude for 10 min. The fraction from 315 to 500 μm was used in this study to minimize digestion differences being a consequence of particle size differences of different batches. The same process was followed for the pure excipients and the blank formulations.

2.3.2. Characterization of the solid lipid-based formulations

The particle size of the powdered LBF mixtures was analyzed via laser diffraction using a Mastersizer 3000 (Malvern Panalytical GmbH, Kassel, Germany) equipped with the Aero S Dispersion Unit (Malvern Panalytical GmbH, Kassel, Germany) at 3 bar dispersion pressure. The data was evaluated based on Fraunhofer theory and x_{10}, x_{50} and x_{90} were calculated to describe the particle size distribution.

To assess the solid state of ritonavir, X-Ray Diffraction (XRD) measurements were carried out with a MiniFlex® 300 (Rigaku, Tokyo, Japan) equipped with a Cu K-α X-ray source set to 15 mA and 40 kV. The step size was 1.7 °/min with an angular range of 2–50° 2θ. Pure ritonavir was measured to identify peaks specific to its crystal structure. Then, measurements were done for each formulation (physical mixture and melted).

Differential scanning calorimetry (DSC) measurements were performed from −20 °C to 200 °C at a heating rate of 10 K/min (1 STARe system, Mettler-Toledo, Germany) for each sLBF to detect the melting range of the formulations.

2.4. Solubility study of ritonavir in the media used in the lipolysis studies

The solubility of ritonavir in the media used during the lipolysis studies was determined using a small-scale shake flask method previously described (Bergström et al., 2002) with slight modifications. An excessive amount of drug (~1.5 mg) was added to 1 mL of FaSSGF or FaSSIF in a centrifuge tube. The suspensions were mixed rapidly and the tubes were shaken by a plate shaker (Schuttler MTS 4 S2 Shaker, IKA-Werke, Staufen im Breisgau, Germany) at 300 rpm and 37 °C. Samples of 100 μL were aliquoted at 24 h, 48 h and 72 h after centrifugation of the tubes at 2300 g and 37 °C for 10 min (Heraeus Megafuge 8R, Thermo Scientific, Waltham, MA, USA). Samples were diluted in ACN (1:1) and kept at −18 °C until analysis with HPLC-UV.

2.5. In vitro intestinal lipolysis studies

2.5.1. Solid lipid excipients

The *in vitro* lipolysis experiments were performed according to the protocol described by Alskär *et al.* (Alskär et al., 2018) Pure excipient powder (1.25 g) was dispersed in 40.56 mL prewarmed (37 °C) FaSSIF medium in the lipolysis vessel for 10 min using a propeller stirrer regulated at approximately 450 rpm. The pH was manually adjusted to 6.5 if the deviation was more than 0.05 pH units. Lipolysis was initiated by the addition of 4.44 mL pancreatin extract. The extract was freshly prepared prior to the experiment by mixing 1.2 g of pancreatin from porcine pancreas with 6 mL of cold lipolysis buffer and centrifuging the mixture at 3500 rpm and 5 °C for 15 min (5810R, Eppendorf, Hamburg, Germany) to remove insoluble pancreatin. The supernatant was used for lipolysis. During the lipolysis, the pH was kept constant at 6.5 by autotitration with 0.6 M NaOH solution (907 Titrando, Metrohm, Herisau, Switzerland) and the temperature was maintained at 37 °C by a circulating water bath. No samples were taken during these experiments. After 60 min of digestion, a step of back-titration to pH 9 was added to evaluate the amount of the unionized free fatty acids that were released during lipolysis. The total amount of FFAs was estimated based on the assumption that the ratio of released ionized and unionized FFAs at 60 min remains constant throughout the experiment. The percentage of total digested fatty acids was calculated based on the saponification values provided by the manufacturers and the assumption that all fatty

Table 2
Composition of solid LBFs (% w/w).

Formulation Name	WITEPSOL® E 85	Gelucire® 48/16	IMWITOR® 491	DYNASAN® 116	Gelucire® 50/13	Ritonavir
Mixture 1 (M1)	45%	45%	–	–	–	10%
Mixture 2 (M2)	35%	35%	20%	–	–	10%
Mixture 3 (M3)	–	–	–	70%	20%	10%

acids can be digested. Lipolysis studies of the blank medium (FaSSIF) were conducted to determine the effect of the medium itself on the consumption of titrant during the experiment. The titration profile of the blank medium was subtracted from the digestion profiles of the excipients (and later formulations).

2.5.2. Solid LBFs

The same protocol was used for the *in vitro* lipolysis studies of the solid ritonavir-loaded LBFs. Samples of 1 mL were taken at predetermined time points (−10, −5, 0, 5, 10, 15, 30, 45, 60 min) without volume replacement and the enzymatic activity was inhibited by the addition of 5 μL of 0.5 M 4-BBBA solution (in methanol) to the sample vials. The samples were then centrifuged at 21,000 g and 37 °C for 15 min (Heraeus Megafuge 8R, Thermo Scientific, Waltham, MA, USA). Complete phase separation was not achieved during this time, and neither when longer centrifugation times were explored. The aqueous phase was therefore aspirated and filtered using Minisart® RC25 syringe filters (pore size 0.2 μm) (Sartorius, Göttingen, Germany). The filtrates were diluted in ACN (1:9) and kept at −18 °C until HPLC-UV analysis.

2.5.3. Solubility study of ritonavir in the aqueous phase during lipolysis

Solid LBFs without ritonavir were digested using the *in vitro* intestinal lipolysis protocol mentioned before. Samples of 2 mL were taken at predetermined time points (0, 10, 30 and 60 min) without volume replacement and 10 μL of 0.5 M 4-BBBA solution (in methanol) were added to stop the activity of the enzyme. The samples were then centrifuged (21,000 g, 37 °C, 15 min) (Heraeus Megafuge 8R, Thermo Scientific, Waltham, MA, USA), the aqueous phase was separated using a syringe and filtered using Minisart® RC25 syringe filters (pore size 0.2 μm) (Sartorius, Göttingen, Germany). For the determination of the drug solubility, a small-scale shake flask method was used. Briefly, 500 μL of the aqueous phase was added to an excessive amount of ritonavir in a tube (triplicate for each time point) and the tubes were shaken at 300 rpm and 37 °C. After 24 h, the tubes were centrifuged at 2300 g and 37 °C for 15 min (Heraeus Megafuge 8R, Thermo Scientific, Waltham, MA, USA) and the supernatants were aliquoted and diluted with ACN (1:9) prior to storage at −18 °C and HPLC-UV analysis.

2.6. In vitro gastrointestinal lipolysis of solid LBFs

The *in vitro* gastrointestinal lipolysis studies were based on a previously reported protocol by Klitgaard *et al.* (Klitgaard et al., 2020) with minor modifications. The sLBF (1.25 g) was dispersed for 2 min in 43 mL prewarmed (37 °C) FaSSGF using a propeller stirrer functioning at approximately 450 rpm. The pH was manually adjusted to 2.5, if the deviation was more than 0.05 pH units. The temperature was kept constant at 37 °C by a circulating water bath. The gastric phase was initiated by the addition of 2 mL of lipase solution, which was prepared by dissolving lipase from *Rhizopus oryzae* in 3 mL cold gastric buffer and centrifuging the solution at 3500 rpm and 5 °C for 15 min (5810R, Eppendorf, Hamburg, Germany). The amount of lipase added was calculated based on its enzymatic activity, in order to reach 50 TBU/mL in the lipolysis vessel. The gastric phase lasted for 30 min and 2 mL samples were aliquoted at predetermined time points (1, 5, 10, 15, 30 min). The activity of the lipase was inhibited by the addition of 10 μL of 0.5 M 4-BBBA solution (in methanol). No titration was recorded during the gastric phase, due to the fact that the free fatty acids released were unionized at the designated pH. Once the gastric phase was over, the pH was automatically adjusted to 6.5 (907 Titrando, Metrohm, Herisau, Switzerland). The consumption of NaOH at this point was used to calculate the amount of free fatty acids released during the gastric phase. Then, 5.56 mL prewarmed (37 °C) concentrated lipolysis medium was added to the vessel and the pH was manually adjusted to 6.5, if the deviation was greater than 0.05 pH units. The addition of 4.44 mL of pancreatin extract (preparation described in 2.5.1.) initiated the intestinal phase of the digestion. The pH was kept constant at 6.5 by autotitration with 0.6 M NaOH solution. Samples (1 mL) were taken at 1, 5, 10, 15, 30, 45, 60 min after the initiation of the intestinal phase without volume replacement and were mixed with 5 μL of 0.5 M 4-BBBA solution (in methanol) to inhibit the lipase activity. All samples were centrifuged at 21,000 g and 37 °C for 15 min (Heraeus Megafuge 8R, Thermo Scientific, Waltham, MA, USA) and, since no complete phase separation occurred, the aqueous phase was filtered using Minisart® RC25 syringe filters (pore size 0.2 μm) (Sartorius, Göttingen, Germany). The filtrates were then diluted in ACN (1:9) and kept at −18 °C until HPLC-UV analysis. Control studies using blank medium were also conducted to determine the amount of NaOH needed for the lipolysis of the components of the medium itself.

2.7. In vitro lipolysis-permeation of solid LBFs

2.7.1. Preparation of the LiDo membrane

The process of preparation of the artificial LiDo (Lecithin in Dodecane) membrane has been reported previously. (Hedge and Bergström, 2020) Briefly, 1 g of lecithin extract was dissolved in 5 mL ethanol: n-dodecane (1.5% v/v ethanol in n-dodecane). The solution was then centrifuged at 3220 g and 20 °C for 20 min (Heraeus Megafuge 8R, Thermo Scientific, Waltham, MA, USA) to separate non-dissolved material from the lecithin solution. The supernatant was aliquoted and frozen at −18 °C until use. The LiDo solution was thawed at room temperature 30 min before the experiment. The membrane was prepared by depositing 713 μL of the solution on a polyvinylidene difluoride (PVDF) filter support (Immobilon®-P Transfer Membrane, 0.45 μm pore size, Millipore, Merck) with a total area of 44 cm^2 (16.2 $\mu L/cm^2$).

2.7.2. Lipolysis-permeation studies

The lipolysis-permeation studies were conducted as described previously by Keemink *et al.* (Keemink et al., 2019) with slight modifications. For these studies, an in-house developed device called the enabling absorption device, ENA for short, was used. This device consists of two compartments; a donor compartment where the LBF is dispersed and digested and a receiver compartment. The two compartments are separated by an artificial membrane, in this case the LiDo membrane, and the temperature of the entire system is kept constant at 37 °C. The receiver compartment was filled with prewarmed (37 °C) PBS (pH 7.4) (~235 mL) supplemented with 0.2% w/v TPGS and homogenization was achieved by magnetic stirring. The donor was filled with 54.08 mL prewarmed (37 °C) FaSSIF (pH 6.5) prepared using a buffer with higher buffering capacity (200 mM TRIS-maleate), as pH measurement and autotitration to maintain the pH stable during digestion was not possible using this setting. (Hedge and Bergström, 2020) Lucifer Yellow (LY) was added at a concentration of 10 μM in the donor chamber to evaluate the integrity of the membrane throughout the experiment. The sLBF (1.5 g) was dispersed for 10 min in the donor compartment using a propeller mixer regulated at ~450 rpm. The digestion was initiated by introducing 5.92 mL of pancreatin extract in the donor chamber. The enzyme extract was freshly prepared 20 min prior to the experiment by mixing 1.6 g of pancreatin from porcine pancreas with 8 mL of cold lipolysis buffer and centrifuging at 3500 rpm and 5 °C for 15 min (5810R, Eppendorf, Hamburg, Germany). The supernatant was kept on ice until use. Samples were taken from both chambers at predetermined time points (0, 5, 15, 30, 45, 60, 90, 120, 150 and 180 min) without volume replacement. Donor samples (750 μL) were treated with 3.75 μL of 0.5 M 4-BBBA solution (in methanol) to inhibit the enzyme activity and were then centrifuged at 21,000 g and 37 °C for 15 min (Heraeus Megafuge 8R, Thermo Scientific, Waltham, MA, USA). The aqueous phase was filtered using Minisart® RC25 syringe filters (pore size 0.2 μm) (Sartorius, Göttingen, Germany). The filtrates were diluted with ACN (1:9) and kept at −18 °C until HPLC-UV analysis. Receiver samples (~300 μL) were split in two and treated differently to detect either LY or ritonavir. For the detection of LY, samples were diluted 1:3

in ACN and centrifuged (21,000 g at 4 °C for 15 min) (Heraeus Megafuge 8R, Thermo Scientific, Waltham, MA, USA) and the supernatants were transferred to a 96-well plate (Costar® black flat bottom, Corning, Kennebunk, ME, USA). For drug quantification, samples were diluted 1:1 with ACN and kept at −18 °C until analysis with HPLC-UV.

2.8. Sample analysis

2.8.1. LY analysis with fluorescence

LY was detected using a plate reader (Spark®, Tecan, Männedorf, Switzerland) in fluorescence mode. Excitation and emission wavelengths were set at 428 nm and 536 nm, respectively.

2.8.2. Ritonavir analysis with HPLC-UV

Ritonavir was quantified using a HPLC-UV system (1290 Infinity, Agilent Technologies, Santa Clara, CA, USA). The column used was a ZORBAX Eclipse XDB-C18 (4.6 × 100 mm, 3.5 μm) (Agilent Technologies, Santa Clara, CA, USA). The temperature was adjusted to 30 °C. An isocratic method with a mobile phase consisting of 45% MilliQ® water and 55% ACN v/v and a flow rate of 0.75 mL/min was used. The injection volume was set at 20 μL and the detection wavelengths used were 210 nm and 240 nm. The retention time was ~5.2 min. Calibration curves were linear ($R^2 > 0.999$) within the range of 0.12–125 μg/mL and the quantified concentrations of quality control samples did not deviate more than 10% from the theoretically calculated concentrations (15% for the lowest concentration). All samples were centrifuged after dilution with ACN at 21,000 g and 22 °C for 15 min (Heraeus Megafuge 8R, Thermo Scientific, Waltham, MA, USA) and the supernatants were used for analysis.

2.9. Data analysis

All experiments were conducted in triplicate. Data are presented as mean values ± standard deviation ($n = 3$). The significance of mean difference was evaluated by one-way ANOVA followed by a *t*-test to determine which pairs of groups were significantly different. The level of significance was set at 0.05. Data manipulation and statistical analysis was conducted on Microsoft Excel, while data visualization and calculations of the areas under the curve (AUCs) were performed in OriginPro 9.0 (OriginLab Corporation).

3. Results and discussion

3.1. Solid LBFs

The formulations in this work were developed based on unpublished prestudies, where different combinations of lipid excipients were spiked with ritonavir and molten under controlled temperature and stirring conditions (60 °C, 25 rpm) for 48 h. DSC measurements from these studies showed that ritonavir was finely dissolved in M1, which is why this formulation was chosen for further experiments. Based on this, formulations M2 and M3 were developed. For M2 the total amount of lipids was increased and supplemented with long chained monoglycerides to see if those could influence the lipolysis and permeation behavior. For M3 long chained triglycerides were used instead of hard fat, since they present higher purity and can potentially influence the solving and dissolution behavior. Gelucire 50/13 was needed to prevent phase separation, due to the fact that Gelucire 48/16 was not miscible with Dynasan 116. According to the LBF classification system introduced by Pouton et al., (Pouton, 2000) all formulations belong to Type II and IIIA.

3.2. Characterization of the solid LBFs

The particle size distributions are shown in Fig. S1 and the x_{10}, x_{50} and x_{90} values and melting range are listed in Table 3. Sieving was the method of choice to isolate a specific particle size fraction (350–500 μm) for all sLBFs in an attempt to minimize differences in the digestion profiles due to size differences of the various batches. However, particle size analysis showed that M2 has a larger particle size (X_{50} = 408 μm) compared to the other two formulations, followed by M1 (X_{50} = 346 μm) and M3 (X_{50} = 285 μm). This has to be considered when interpreting digestion data as smaller particles present larger surface area accessible for digestion.

Table 3
X_{10}, X_{50} and X_{90} values and melting range of the solid LBFs.

	M1	M2	M3
X_{10} (μm)	88	246	83.8
X_{50} (μm)	346	408	285
X_{90} (μm)	575	621	515
Melting range (°C)	31 - 47	22 - 65	41 - 62

The XRD results are presented in Fig. S2 which can be found in the Supplementary Information. Isolated peaks of ritonavir were found from 8° to 11° and are highlighted in the graph. Other peaks are overlayed by the crystal structures of the matrices. By comparing the data from the physical mixtures of each formulation to the melted LBFs, it is observed that the crystalline amount of ritonavir is reduced in all formulations. However, small peaks of ritonavir can be detected in all spectra of molten LBFs, meaning that small amounts of ritonavir remain crystalline. This may influence the stability of the LBFs, as it could possibly accelerate the recrystallisation of ritonavir in the formulation. However, ritonavir shows slow recrystallization, even in the presence of crystalline traces, (Law et al., 2001) and so the effect of crystalline tracers may be limited. Further stability studies need to be conducted to investigate the long term stability of these LBFs.

3.3. Solubility of ritonavir

The solubility of ritonavir was determined in the media used during the *in vitro* lipolysis studies and in the aqueous phase during the digestion of the three different mixtures (Fig. 1). The solubility in FaSSIF was found to be lower (4.0 ± 0.2 μg/mL) compared to the solubility in FaSSGF (8.38 ± 1.91 μg/mL) (Fig. 1A). This was expected since ritonavir is a weak diprotic base (pKa values 1.8 and 2.6) (Velozo et al., 2022) and presents pH dependent solubility with higher solubility under acidic conditions. (Fiolka et al., 2020) Further, the solubility of ritonavir in the aqueous phase is higher when LBFs are present compared to the blank medium (FaSSIF). However, it decreases over time as the digestion of the sLBFs progresses (Fig. 1B); the solubility of ritonavir is negatively correlated to the amount of the digestion products of M1 and M2 present in the aqueous phase. In the case of M3, an initial increase of the solubility of ritonavir in the aqueous phase is noted, but as digestion progresses the solubility decreases similarly to M1 and M2.

3.4. In vitro lipolysis of the solid lipid excipients

The results from the *in vitro* digestion studies of the pure solid lipid excipients are presented in Fig. 2. The ionized fraction of the FFAs released was calculated based on the consumption of NaOH during digestion. The digestion of the blank medium (FaSSIF) has been considered and deducted in all cases. The unionized fraction of the FFAs released during digestion was determined by quick back titration to pH 9 at the end of each experiment, while also considering the amount of NaOH needed for the blank medium. Witepsol E85 presented the highest digestibility among the excipients studied, releasing high amounts of both ionized and unionized FFAs (up to approximately 48% of the theoretical total fatty acids). This was expected as Witepsol excipients are hard fats consisting mainly of glycerol esters of saturated fatty acids. The excipients that followed with significantly lower amounts of FFAs released were Gelucires, containing esters of polyethylene glycol with

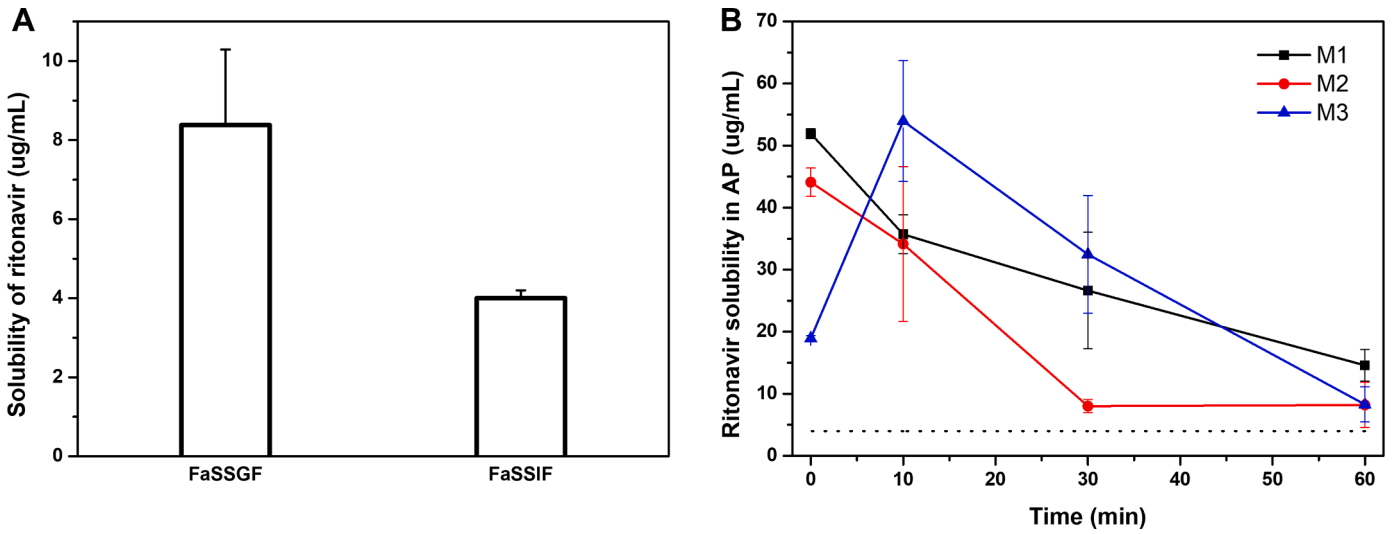

Fig. 1. (A) Solubility of ritonavir in the biorelevant media of the *in vitro* lipolysis studies. (B) Solubility of ritonavir in the aqueous phase (AP) during *in vitro* lipolysis studies. The dashed lined indicates the equilibrium solubility of ritonavir in FaSSIF. Data are presented as mean values ± standard deviation ($n = 3$).

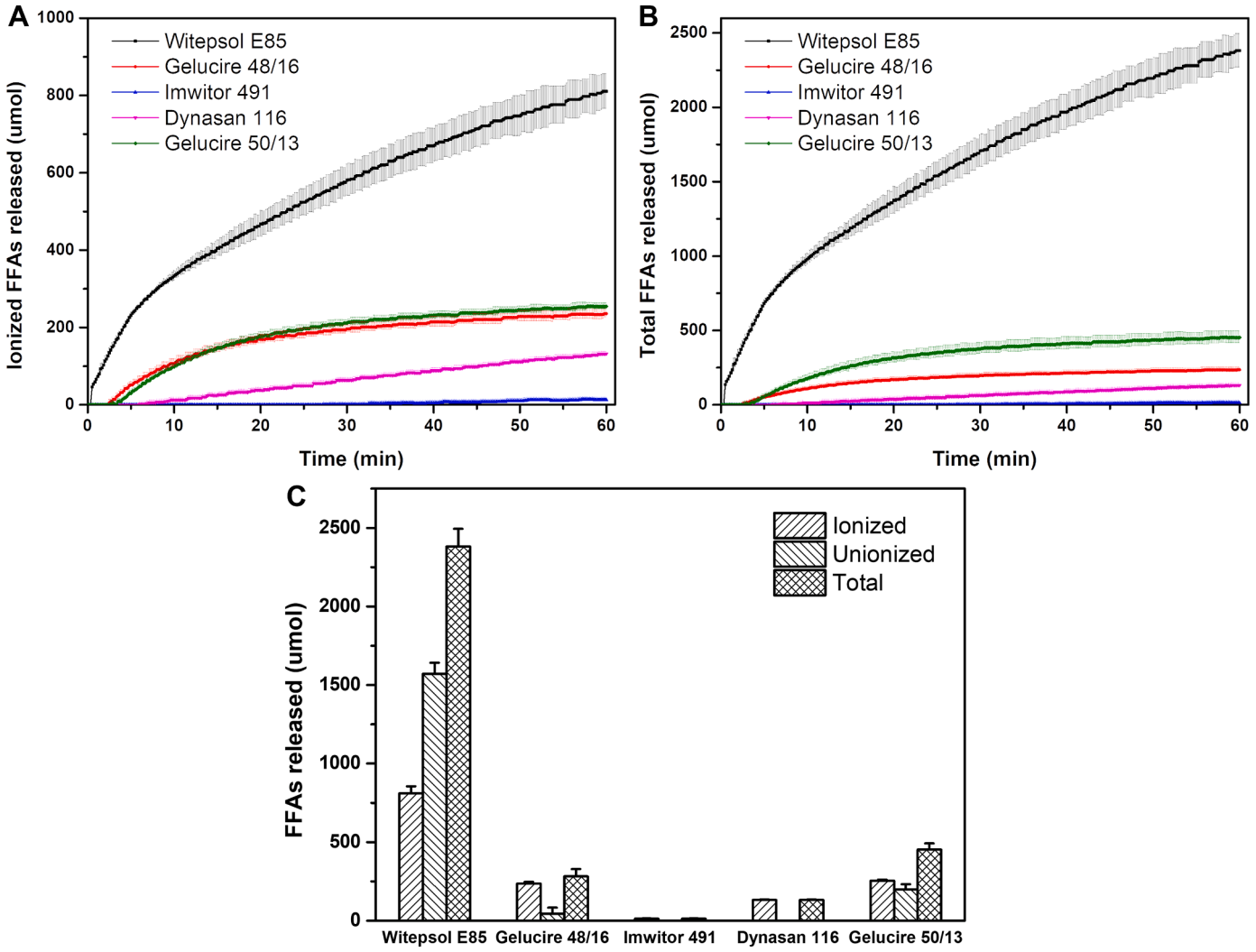

Fig. 2. Free fatty acids (FFAs) released during the *in vitro* intestinal lipolysis studies of the solid lipid excipients. (A) The ionized FFAs released were calculated based on the autotitration with NaOH by correcting the values through subtraction of the digestion of the blank medium. (B) and (C) The unionized fraction of FFAs released was calculated by the backtitration step to pH 9 at the end of the experiment. The total FFAs released were estimated by assuming that the ratio of ionized and unionized FFAs at 60 min remains constant throughout the duration of the experiments.

palmitic and stearic acid. Gelucire 50/13 released a higher total amount of FFAs (around 28% of its theoretical total fatty acids) compared to Gelucire 48/16 (around 36% of its theoretical total fatty acids), a consequence of that Gelucire 50/13 also contains mono-, di- and triglycerides. Even though Dynasan 116 is a triglyceride (glyceryl tripalmitate), only a small amount of ionized FFAs was released (2.8% of the fatty acidss that could be digested), possibly due to its solid nature. This is in agreement with a study by Witzleb *et al.*, (Witzleb et al., 2012) where glyceryl tripalmitate was digested only up to 10% after 80 min. No unionized fraction was detected as palmitic acid has a pKa of 4.75 and the FFAs released are expected to be fully ionized at pH 6.5. Imwitor 491 appears to be practically indigestible (0.4% digested fatty acidss), possibly due to its solid state and poor solubility in the aqueous medium (HLB ~ 4). The stereoisomer used in this study (1-monostearate or 2-monostearate) is not known and therefore the stereoselective activity of the pancreatic lipase might also play a role, since the excipient contains more than 90% monoglycerides (glyceryl monostearate) and the pancreatic lipase is known to have low activity against 2-monoglycerides.

3.5. Intestinal lipolysis of ritonavir-loaded solid LBFs

The digestion of the drug loaded sLBFs was studied *in vitro* using a well-established protocol, which imitates the lipid digestion process in the intestine in the fasted state (Fig. 3). The ionized FFAs released during the 60 min experiments were calculated based on the amount of NaOH used for the auto-titration step by subtracting the amount of NaOH needed for the digestions of the blank medium (FaSSIF) (Fig. 3A). M1 and M3 were digested to the same extent (around 8% and 5% of the theoretical total fatty acids, respectively) but M3 had a slower rate of digestion than M1. M2 presents higher and faster digestion (up to 36%) compared to M1, probably due to the presence of Imwitor 491 in its composition, which acts as a non-ionic co-emulsifier (HLB value ~4) and enables the digestion of the main digestible excipient (*i.e.*, Witepsol E85). This is also supported by the fact that M2 released a much higher amount of unionized FFAs, as expected for the digestion of the hard fat. Even though the same response to digestion would be expected for M1, as it contains a high amount of Witepsol E85, the low fraction of unionized FFAs leads to the assumption that the digestion of M1 is mainly attributed to Gelucire 48/16 due to its higher water solubility and not to Witepsol E85. In order to verify this assumption, the experiment was repeated for all three formulations, but for an extended period of time (180 min) (Fig. 3C and D). From this experiment, it becomes evident that all formulations are digested in a bimodal manner with M2 presenting the highest digestibility (up to 58% in 3 h) and M3 the lowest (up to 18% in 3 h) after full duration of the experiment. Since M1 released a high amount of unionized FFAs after 180 min (reaching approximately 46% digestion of its theoretical total fatty acids), it can be presumed that the digestion of Witepsol E85 in M1 is delayed by the presence of Gelucire 48/16, which is digested initially due to its higher solubility. In the case of M3, the unionized fraction of FFAs is also higher after 180 min. This fraction can only be attributed to the digestion of Gelucire 50/13, as Dynasan 116 did not exhibit an unionized fraction of released FFAs during the digestion experiments of the pure excipient. This may be explained by the low percentage of Gelucire 50/13 in the composition of M3 compared to Dynasan 116. Overall, the digestibility of the sLBFs is mostly affected by their composition, while the differences in particle size are not directly influencing the rate or the extent of the digestion.

The distribution of ritonavir could not be studied in all three phases of the sample withdrawn (oil, aqueous and pellet phase) as it was not possible to effectively separate them by centrifugation. The aqueous phase was aliquoted and filtered and the concentration of ritonavir was determined throughout the digestion experiment (Fig. 3E). During the 10 min dispersion phase -before the initiation of digestion- the concentration is increasing for all formulations, possibly due to the dissolution of the sLBFs. The high variability noted in this phase might be the result of poor dispersibility of the sLBFs in the medium and may potentially be overcome by increasing the duration of the dispersion phase when working with sLBFs. Nevertheless, it seems that M1 and M2 can achieve higher aqueous ritonavir concentrations compared to M3. Once digestion starts, ritonavir concentration decreases for all three formulations due to precipitation, until finally reaching a plateau close to the equilibrium solubility of ritonavir in FaSSIF. M2 seems to present the fastest precipitation of ritonavir possibly linked to the faster digestion rate and more rapid loss of solubilization (Fig. 3A). Comparing these profiles to the results from the solubility study of ritonavir in the aqueous phase, it can be observed that these formulations can only maintain supersaturation briefly after the initiation of the digestion and precipitation prevails. To evaluate the performance of the proposed formulations, the AUCs of the ritonavir concentration profiles over time were calculated and compared (Fig. 3F). No statistically significant differences were observed among the three different mixtures.

3.6. Gastrointestinal lipolysis of ritonavir-loaded solid LBFs

A two-step *in vitro* gastrointestinal digestion model was also implemented to evaluate the performance of the drug-loaded sLBFs (Fig. 4). During the gastric phase, even though the pH was monitored and stable at 2.5, auto-titration was not possible to use to determine the released FFA as any FFAs would be unionized at the designated pH. Thus, the amount of FFAs released during the gastric step was determined by a fast titration step from pH 2.5 to pH 6.5 at the end of the 30 min gastric phase (Fig. 4A). The gastric digestion of the sLBFs is low, as expected due to the low activity of the lipase used for this step. However, rapid release of FFAs can be observed during the intestinal phase (Fig. 4B), with M2 presenting the highest digestibility, followed by M1 and M3. Based on the composition of the sLBFs and the digestion experiments of the pure excipients, this ranking was anticipated. M1 and M2 contain a highly digestible hard fat (Witepsol E85) but M2 also contains a co-emulsifier (Imwitor 491) that assists the dispersion and/or emulsification of the hard fat, making it more accessible for digestion. Contrasting the digestion profiles of M1 and M2 to those of the intestinal lipolysis experiments, digestion starts much faster and more ionized FFAs are released in a unimodal way when the gastrointestinal lipolysis is used. This means that the addition of the gastric step helps the dispersibility/dissolution of these sLBFs through the low pH, addition of another type of lipase and the longer dispersion time that is used. The addition of another enzyme in the gastric lipolysis might also assist the digestion or even boost the activity of the pancreatic lipase when moving to the intestinal stage. (Klitgaard et al., 2020) Nevertheless, a clearer ranking of the sLBFs in terms of digestibility is achieved by using the gastrointestinal protocol.

The concentration of ritonavir in the aqueous phase throughout the gastrointestinal lipolysis experiments is presented in Fig. 4C. During the gastric step, M1 and M2 provided a much higher solubilization of ritonavir compared to M3, while a slight decrease of concentration over time was observed, possibly due to digestion of the sLBFs. Since high concentrations of ritonavir are achieved rapidly, it is assumed that the duration of the gastric phase is not the main factor causing the improved dispersion of the sLBFs. Thus, the low pH seems to be the leading cause for the higher solubilization capacity. Once the intestinal phase is initiated, a fast decrease in the concentration of ritonavir can be observed, due to that the change in pH and increased digestion of the sLBFs both trigger precipitation of ritonavir. During the intestinal phase, M1 and M2 reach a stable concentration that is 5 to 7 times higher compared to M3. However, considering the total AUC of the concentration profiles, M1 performs the best among the three different sLBFs. Klitgaard et al. showed that the *in vitro* gastrointestinal digestion model not only provided a clearer ranking of two liquid LBFs tested in their study, but also correctly predicted their *in vivo* performance in dogs by rank order, something the intestinal model failed to achieve. (Klitgaard

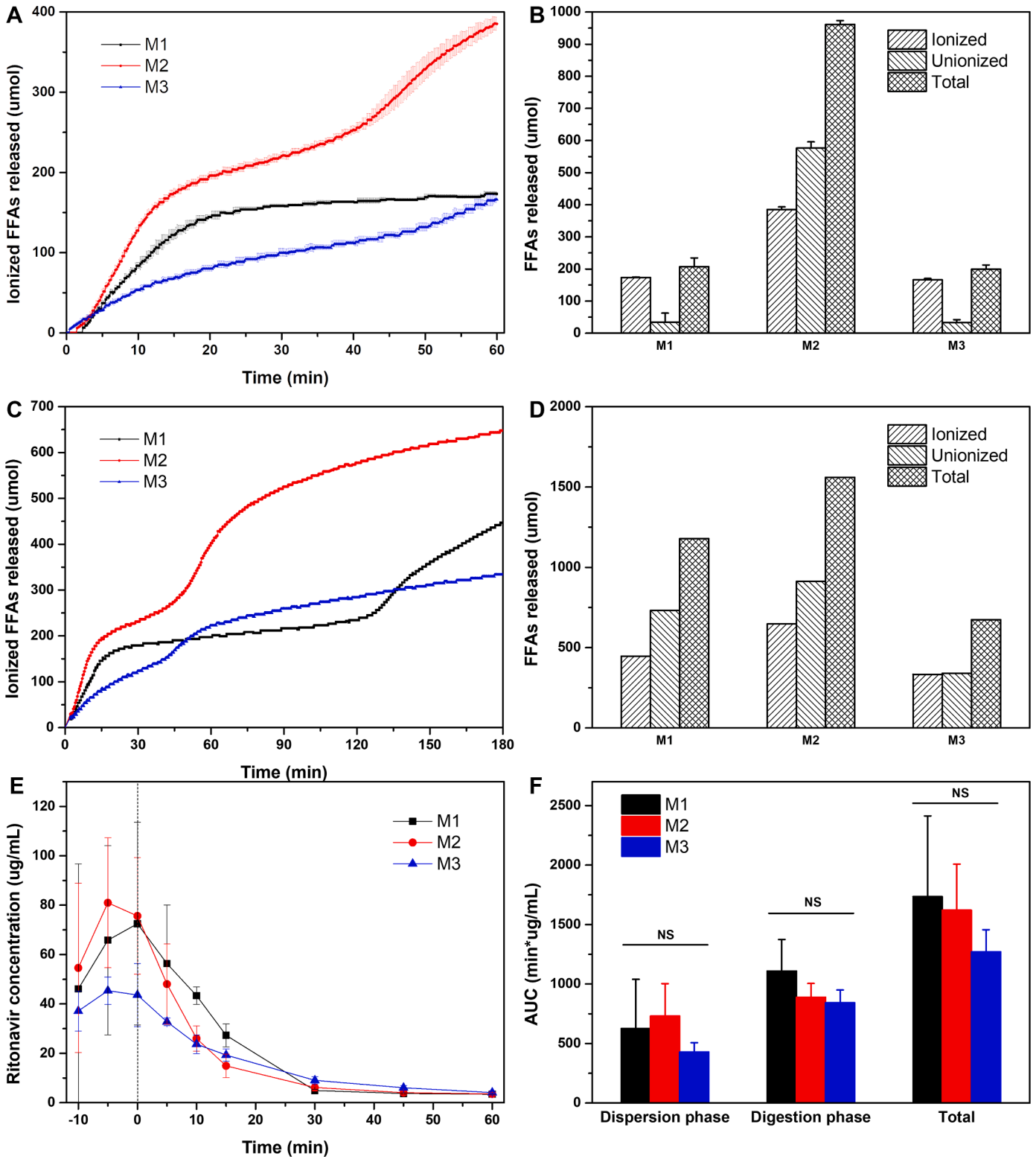

Fig. 3. *In vitro* intestinal lipolysis of solid LBFs. Figures C-D represent single experiments ($n = 1$). (A) Ionized FFAs released during the intestinal lipolysis experiments. (B) Amounts of FFAs released after 60 min of digestion of the solid LBFs. (C) Ionized FFAs released during the 180 min digestion experiment. (D) Amounts of FFAs released after 180 min of digestion of the solid LBFs. (E) Concentration of ritonavir in the aqueous phase during the *in vitro* intestinal lipolysis of the solid LBFs. The dotted line indicates the end of the dispersion phase and the beginning of the digestion. (F) Aqueous ritonavir concentration over time profiles presented as area under the curve (AUC) for the three different solid LBFs. (NS= no statistical significance).

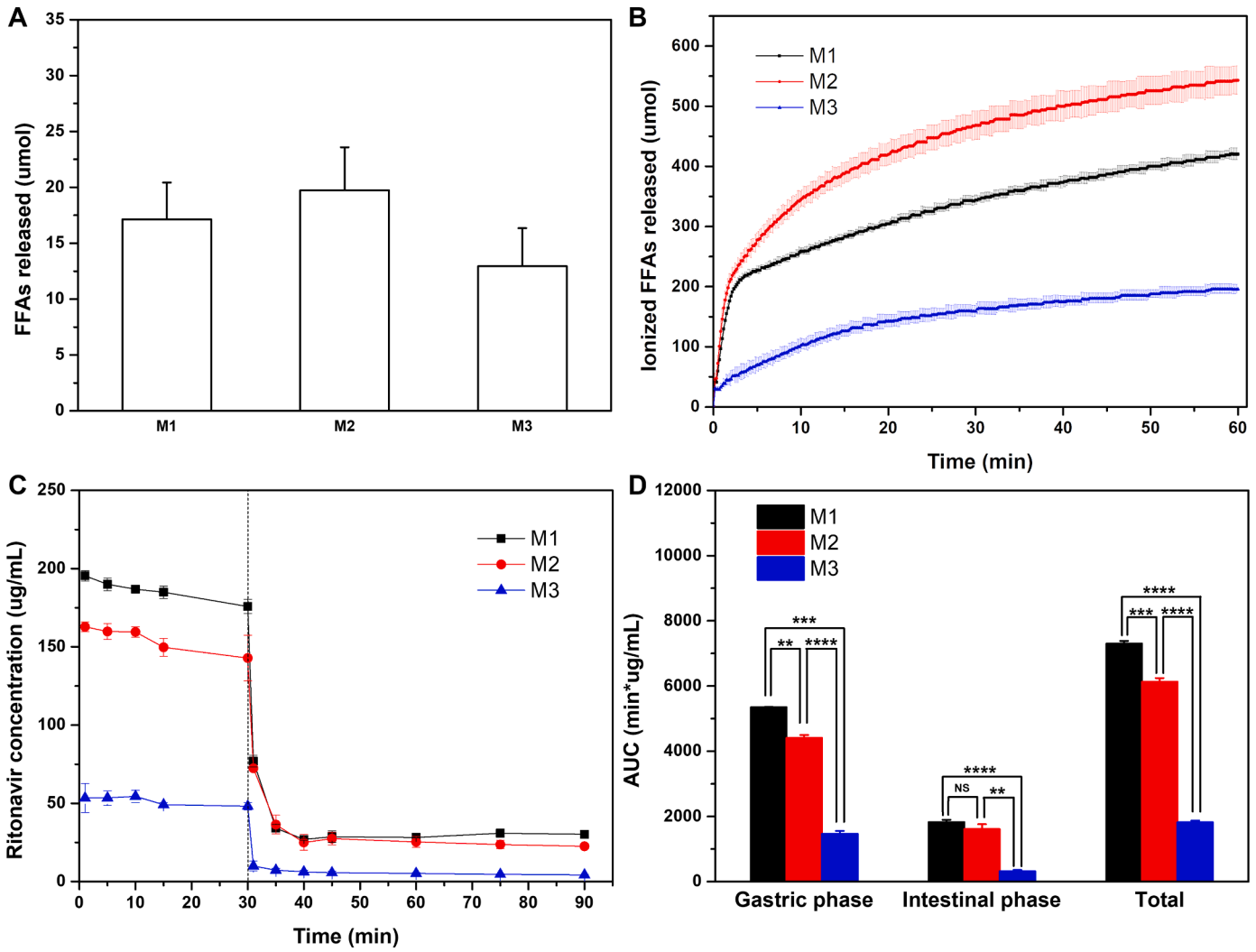

Fig. 4. *In vitro* gastrointestinal lipolysis of solid LBFs. (A) Amounts of FFAs released during the gastric phase of the gastrointestinal lipolysis experiments. (B) Ionized FFAs released during the intestinal phase of the gastrointestinal lipolysis experiments. (C) Concentration of ritonavir in the aqueous phase during the *in vitro* gastrointestinal lipolysis of the solid LBFs. The dotted line indicates the end of the gastric phase and the beginning of the intestinal phase. (D) Exposure of ritonavir over time presented as area under the curve (AUC) for the three different solid LBFs. Asterisks indicate the level of statistical significance (**$p < 0.01$, ***$p < 0.001$ and ****$p < 0.0001$) (NS= no statistical significance).

et al., 2020) However, in their study only two formulations were explored and further studies are needed to prove the gastrointestinal model indeed is more predictive for absorption to the systemic circulation.

3.7. Lipolysis and permeation studies of ritonavir-loaded solid LBFs

The effect of the three different sLBFs on the permeability of ritonavir was evaluated in parallel to their digestion using an in-house device consisting of a donor and a receiver chamber (Fig. 5). In the donor compartment the sLBFs are digested by the pancreatic lipase and the concentration of ritonavir in the aqueous phase is decreasing in a similar way to the *in vitro* intestinal digestion studies (Fig. 5A). M1 manages to maintain a higher concentration of ritonavir in the aqueous phase for most time points compared to M2 (not statistically significant) and M3. However, in this case the inferior performance of M3 is more evident and the ranking of the three sLBFs is more distinct. Additionally, less variability was observed for each formulation when this set-up was used, probably due to the improved dispersion of the sLBFs in the donor chamber compared to the vessel used for the *in vitro* intestinal digestion studies. An interesting observation was made after 90 min, when the concentration of ritonavir for M1 and M2 increases in the donor chamber possibly due to re-solubilization of the precipitated ritonavir. Based on a study by Alskär et al., (Alskär et al., 2018) molecules with specific physicochemical characteristics (*i.e.*, molecular weight > 350 g/mol and melting point < 200 °C) tend to form amorphous precipitates when presented in a supersaturated environment. Ritonavir meets the abovementioned criteria (molecular weight 720.9 g/mol and melting point ~ 124 °C (Sinha et al., 2010)). Tanaka et al. also proved that amorphous ritonavir precipitated during the *in vitro* digestion studies of Type IIIB-MC and Type IV LBFs. They claimed that this may contribute to the re-solubilization of the precipitated drug and the improved oral absorption. (Tanaka et al., 2021)

Ritonavir was also detected and quantified in samples from the receiver compartment (Fig. 5B). The drug flux seems to be stable over time, not being majorly affected by the concentration of ritonavir in the donor chamber. The permeation profiles are linear and the three LBFs enable the permeability of ritonavir in a similar manner, but when comparing the AUCs (Fig. 5C), M1 appears to perform best followed by M2 and M3. The difference between the AUCs of M1 and M3 is statistically significant, due to the greater difference in ritonavir permeated after the first 90 min of the experiment. It is noteworthy that the LiDo membrane remained intact throughout the duration of the experiments in all cases, as no LY was detected in the receiver compartment (data not

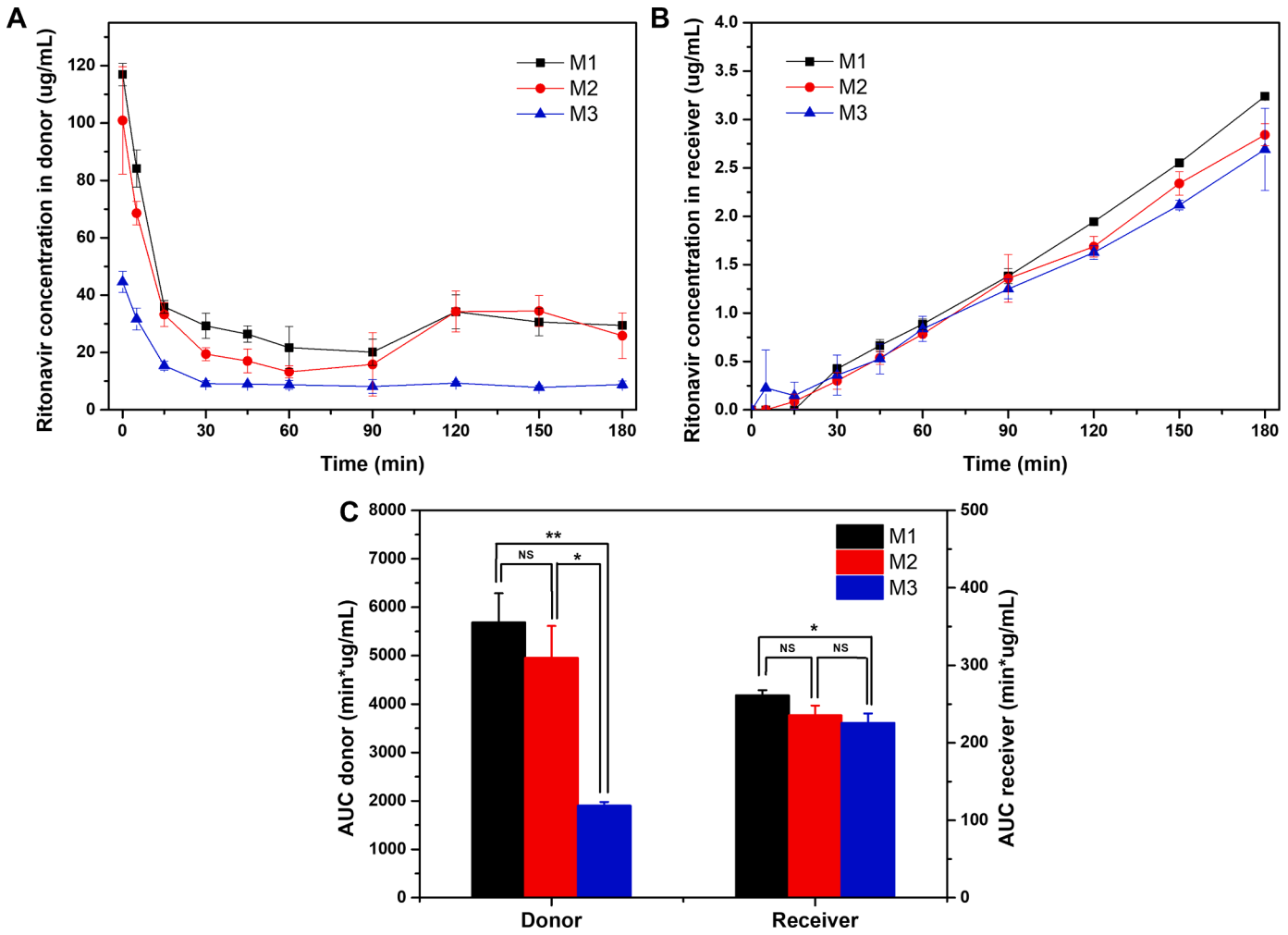

Fig. 5. *In vitro* lipolysis-permeation studies of solid LBFs. Data are presented as mean values ± standard deviation ($n = 3$). (A) Concentration of ritonavir in the aqueous phase in the donor compartment over time. (B) Concentration of ritonavir in the receiver compartment over time. (C) Area-under-the-curve (AUC) for the three different solid LBFs for both compartments. Asterisks indicate the level of statistical significance (*$p < 0.05$ and **$p < 0.01$) (NS= no statistical significance).

shown). It has been suggested previously that higher amounts of excipients can either increase the permeability of lipophilic drugs through the intestine due to increased solubilization or decrease it due to reduced thermodynamic activity. (Tanaka et al., 2022) In this study, the increased solubilization of ritonavir in the donor chamber for two of the sLBFs does not seem to significantly affect permeation, and this may be explained by the high amounts of excipients used for the formulations tested. The data is also in line with the study of Tanaka et al., (Tanaka et al., 2022) in which is mentioned that apparent permeability may play a more important role in the absorption of ritonavir compared to drug solubilization, even though lipid digestion and monitoring of the concentration of the drug available for absorption remain key factors for the assessment and prediction of LBF performance and drug absorption.

Most current models do not evaluate digestion and permeation simultaneously, but rather make use of two separate assays; the first one is the digestion step represented by the usual pH-stat lipolysis model and then the contents are transferred to another set-up for the second step, *i.e.*, the permeation step. (Berthelsen et al., 2019) The systems that have been used for the permeation step till date are Ussing chambers, (Bibi et al., 2017) Transwell systems (Keemink and Bergström, 2018) and Franz diffusion cells. (Klitgaard et al., 2021) Others tried to combine the *in vitro* digestion studies with *ex vivo* permeation studies using rat small intestine sections as the barrier between the side-by-side Ussing chambers (Dahan and Hoffman, 2007) or with *in situ* perfusion studies in anaesthetized rat. (Crum et al., 2016) The ENA used in this study is the first experimental set-up designed to simultaneously test the digestion of LBFs and the permeation of the API *in vitro*. (Keemink et al., 2019) This device has previously only been used to study liquid LBFs and was herein for the first time used to study flux of sLBFs. The results support the suitability and flexibility of the system for investigating solid formulations as well. Recently, another *in vitro* model for the simultaneous evaluation of lipolysis and permeation of LBFs using a mucus-PVPA barrier and a Transwell system was presented by Falavigna *et al.* (Falavigna et al., 2021) In that study, the presence of an absorption chamber proved once more to be beneficial for the IVIVC when it comes to the evaluation of LBFs. However, that system was limited to the evaluation of liquid LBFs. Furthermore, no experimental set-ups have been reported so far for the combined *in vitro* gastrointestinal lipolysis of LBFs and intestinal permeation, which would definitely provide further physiological relevance and valuable data during the development and optimization of all types of LBFs.

Although *e.g.* the ENA has proven to produce *in vivo* relevant data for different drugs and in different species, the data produced in this study was not generated with the purpose to predict *in vivo* performance *per se* and have not been correlated to the performance of these sLBFs *in vivo*. The tools were herein used as guides to make better informed decisions for the selection and optimization of sLBFs during the development phase.

4. Conclusions

Solid LBFs are an advantageous formulation strategy for lipophilic drug substances, but the need for suitable methodologies for the complete evaluation of their performance *in vitro* has still not been met. This work is the first attempt to modify existing methods mostly optimized for liquid formulation in order to satisfy this need. While the classic *in vitro* intestinal digestion assay fails to provide a clear ranking of the performance of the three sLBFs tested, the two modified and more physiologically relevant *in vitro* assays seem more suitable for studies of performance of sLBFs. The two-step gastrointestinal digestion assay captures the performance of those LBFs in the acidic environment of the stomach, of great importance to formulations of weak bases. Further, the *in vitro* digestion-permeability assay was successfully used for the first time to study sLBFs and provided information about the solubilization capacity of the donor solution during digestion of sLBFs and to what extent that is linked to a higher flux across an artificial membrane. Based on the results from the modified *in vitro* tools used in this study, M1 supports greater absorption than do the other two formulations and will be subject to further exploration and optimization.

Funding source

The Swedish Research council grant 2018-03281

CRediT authorship contribution statement

Ioannis I. Andreadis: Conceptualization, Methodology, Investigation, Formal analysis, Data curation, Writing – original draft. **Arne Schulzen:** Conceptualization, Methodology, Investigation, Writing – original draft. **Julian Quodbach:** Conceptualization, Methodology, Writing – review & editing, Funding acquisition. **Christel A.S. Bergström:** Conceptualization, Methodology, Writing – review & editing, Funding acquisition.

Declaration of Competing Interest

Ioannis I. Andreadis is currently an employee of AstraZeneca PLC. Christel A. S. Bergström is founder of the company Enphasys AB, which holds the patent for the ENA device.

Data availability

Data will be made available on request.

Acknowledgments

The authors would like to thank Dr. Tobias Auel for his assistance with the XRD measurements.

Supplementary materials

Supplementary material associated with this article can be found, in the online version, at doi:10.1016/j.ejps.2023.106524.

References

Alskär, L.C., Keemink, J., Johannesson, J., Porter, C.J.H., Bergström, C.A.S., 2018. Impact of drug physicochemical properties on lipolysis-triggered drug supersaturation and precipitation from lipid-based formulations. Mol. Pharmaceut. 15 (10), 4733–4744. https://doi.org/10.1021/acs.molpharmaceut.8b00699.

Bergström, C.A.S., Norinder, U., Luthman, K., Artursson, P., 2002. Experimental and computational screening models for prediction of aqueous drug solubility. Pharm. Res. 19 (2), 182–188. https://doi.org/10.1023/A:1014224900524.

Berthelsen, R., Klitgaard, M., Rades, T., Müllertz, A., 2019. In vitro digestion models to evaluate lipid based drug delivery systems; present status and current trends. Adv. Drug Deliv. Rev. 142, 35–49. https://doi.org/10.1016/j.addr.2019.06.010.

Bibi, H.A., Holm, R., Bauer-Brandl, A., 2017. Simultaneous lipolysis/permeation in vitro model, for the estimation of bioavailability of lipid based drug delivery systems. Eur. J. Pharmaceut. Biopharmaceut. 117, 300–307. https://doi.org/10.1016/j.ejpb.2017.05.001.

Carrière, F., 2016. Impact of gastrointestinal lipolysis on oral lipid-based formulations and bioavailability of lipophilic drugs. Biochimie 125, 297–305. https://doi.org/10.1016/j.biochi.2015.11.016.

Chabni, A., Bañares, C., Reglero, G., Torres, C.F., 2022. A comparative study of in vitro gastrointestinal digestion of three strategic edible oils. J. Food Sci. 87 (7), 3268–3278. https://doi.org/10.1111/1750-3841.16212.

Chatzidaki, M.D., Mateos-Diaz, E., Leal-Calderon, F., Xenakis, A., Carrière, F., 2016. Water-in-oil microemulsions *versus* emulsions as carriers of hydroxytyrosol: an in vitro gastrointestinal lipolysis study using the PHstat technique. Food Funct. 7 (5), 2258–2269. https://doi.org/10.1039/C6FO00361C.

Christophersen, P.C., Christiansen, M.L., Holm, R., Kristensen, J., Jacobsen, J., Abrahamsson, B., Müllertz, A., 2014. Fed and fasted state gastro-intestinal in vitro lipolysis: in vitro in vivo relations of a conventional tablet, a SNEDDS and a solidified SNEDDS. Eur. J. Pharmaceut. Sci. 57, 232–239. https://doi.org/10.1016/j.ejps.2013.09.007.

Crum, M.F., Trevaskis, N.L., Williams, H.D., Pouton, C.W., Porter, C.J.H, 2016. A new in vitro lipid digestion – in vivo absorption model to evaluate the mechanisms of drug absorption from lipid-based formulations. Pharm. Res. 33 (4), 970–982. https://doi.org/10.1007/s11095-015-1843-7.

Dahan, A., Hoffman, A., 2007. The effect of different lipid based formulations on the oral absorption of lipophilic drugs: the ability of in vitro lipolysis and consecutive ex vivo intestinal permeability data to predict in vivo bioavailability in rats. Eur. J. Pharmaceut. Biopharmaceut. 67 (1), 96–105. https://doi.org/10.1016/j.ejpb.2007.01.017.

Falavigna, M., Brurok, S., Klitgaard, M., Flaten, G.E., 2021. Simultaneous assessment of in vitro lipolysis and permeation in the mucus-PVPA model to predict oral absorption of a poorly water soluble drug in SNEDDSs. Int. J. Pharm. 596, 120258 https://doi.org/10.1016/j.ijpharm.2021.120258.

Feeney, O.M., Crum, M.F., McEvoy, C.L., Trevaskis, N.L., Williams, H.D., Pouton, C.W., Charman, W.N., Bergström, C.A.S., Porter, C.J.H, 2016. 50 years of oral lipid-based formulations: provenance, progress and future perspectives. Adv. Drug Deliv. Rev. 101, 167–194. https://doi.org/10.1016/j.addr.2016.04.007.

Fernandez, S., Chevrier, S., Ritter, N., Mahler, B., Demarne, F., Carrière, F., Jannin, V., 2009. In vitro gastrointestinal lipolysis of four formulations of piroxicam and cinnarizine with the self emulsifying excipients Labrasol® and Gelucire® 44/14. Pharm. Res. 26 (8), 1901–1910. https://doi.org/10.1007/s11095-009-9906-2.

Fernandez, S., Jannin, V., Chevrier, S., Chavant, Y., Demarne, F., Carrière, F., 2013. In vitro digestion of the self-emulsifying lipid excipient Labrasol® by gastrointestinal lipases and influence of its colloidal structure on lipolysis rate. Pharm. Res. 30 (12), 3077–3087. https://doi.org/10.1007/s11095-013-1053-0.

Fiolka, T., Van Den Abeele, J., Augustijns, P., Arora, S., Dressman, J., 2020. Biorelevant two-stage in vitro testing for RDCS classification and in PBPK modeling–case example ritonavir. J. Pharm. Sci. 109 (8), 2512–2526. https://doi.org/10.1016/j.xphs.2020.04.023.

Hedge, O.J., Bergström, C.A.S., 2020. Suitability of artificial membranes in lipolysis-permeation assays of oral lipid-based formulations. Pharm. Res. 37 (6), 99. https://doi.org/10.1007/s11095-020-02833-9.

Keemink, J., Bergström, C.A.S, 2018. Caco-2 cell conditions enabling studies of drug absorption from digestible lipid-based formulations. Pharm. Res. 35 (4), 74. https://doi.org/10.1007/s11095-017-2327-8.

Keemink, J., Hedge, O.J., Bianco, V., Hubert, M., Bergström, C.A.S, 2022. Comparison of cellular monolayers and an artificial membrane as absorptive membranes in the in vitro lipolysis-permeation assay. J. Pharm. Sci. 111 (1), 175–184. https://doi.org/10.1016/j.xphs.2021.09.009.

Keemink, J., Mårtensson, E., Bergström, C.A.S, 2019. Lipolysis-permeation setup for simultaneous study of digestion and absorption in vitro. Mol. Pharmaceut. 16 (3), 921–930. https://doi.org/10.1021/acs.molpharmaceut.8b00811.

Klitgaard, M., Beilles, S., Sassene, P.J., Berthelsen, R., Müllertz, A., 2020. Adding a gastric step to the intestinal *in vitro* digestion model improves the prediction of pharmacokinetic data in beagle dogs of two lipid-based drug delivery systems. Mol. Pharmaceut. 17 (9), 3214–3222. https://doi.org/10.1021/acs.molpharmaceut.0c00307.

Klitgaard, M., Müllertz, A., Berthelsen, R., 2021. Estimating the oral absorption from self-nanoemulsifying drug delivery systems using an in vitro lipolysis-permeation method. Pharmaceutics 13 (4), 489. https://doi.org/10.3390/pharmaceutics13040489.

Law, D., Krill, S.L., Schmitt, E.A., Fort, J.J., Qiu, Y., Wang, W., Porter, W.R., 2001. Physicochemical considerations in the preparation of amorphous ritonavir–Poly (Ethylene Glycol) 8000 solid dispersions. J. Pharm. Sci. 90 (8), 1015–1025. https://doi.org/10.1002/jps.1054.

Pouton, C.W., 2000. Lipid formulations for oral administration of drugs: non-emulsifying, self-emulsifying and 'self-microemulsifying' drug delivery systems. Eur. J. Pharmaceut. Sci. 11, S93–S98. https://doi.org/10.1016/S0928-0987(00)00167-6.

Rossi, R.C., Dias, C.L., Donato, E.M., Martins, L.A., Bergold, A.M., Fröehlich, P.E., 2007. Development and validation of dissolution test for ritonavir soft gelatin capsules based on in vivo data. Int. J. Pharm. 338 (1–2), 119–124. https://doi.org/10.1016/j.ijpharm.2007.01.036.

Sams, L., Paume, J., Giallo, J., Carrière, F., 2016. Relevant PH and lipase for in vitro models of gastric digestion. Food Funct. 7 (1), 30–45. https://doi.org/10.1039/C5FO00930H.

Silva, L.A.D., Almeida, S.L., Alonso, E.C.P., Rocha, P.B.R., Martins, F.T., Freitas, L.A.P., Taveira, S.F., Cunha-Filho, M.S.S., Marreto, R.N., 2018. Preparation of a solid self-

microemulsifying drug delivery system by hot-melt extrusion. Int. J. Pharm. 541 (1–2), 1–10. https://doi.org/10.1016/j.ijpharm.2018.02.020.

Sinha, S., Ali, M., Baboota, S., Ahuja, A., Kumar, A., Ali, J., 2010. Solid dispersion as an approach for bioavailability enhancement of poorly water-soluble drug ritonavir. AAPS PharmSciTech 11 (2), 518–527. https://doi.org/10.1208/s12249-010-9404-1.

Tanaka, Y., Doi, H., Katano, T., Kasaoka, S., 2021. Effects of lipid digestion and drug permeation/re-dissolution on absorption of orally administered ritonavir as different lipid-based formulations. Eur. J. Pharmaceut. Sci. 157, 105604 https://doi.org/10.1016/j.ejps.2020.105604.

Tanaka, Y., Doi, H., Katano, T., Kasaoka, S., 2022. The impact of quantity of lipid based formulations with different compositions on the oral absorption of ritonavir: a trade-off between apparent solubility and permeability. Eur. J. Pharmaceut. Sci. 168, 106079 https://doi.org/10.1016/j.ejps.2021.106079.

Van Speybroeck, M., Williams, H.D., Nguyen, T.-H., Anby, M.U., Porter, C.J.H., Augustijns, P., 2012. Incomplete desorption of liquid excipients reduces the *in vitro* and *in vivo* performance of self-emulsifying drug delivery systems solidified by adsorption onto an inorganic mesoporous carrier. Mol. Pharmaceut. 9 (9), 2750–2760. https://doi.org/10.1021/mp300298z.

Velozo, C.T., Cabral, L.M., Pinto, E.C., de Sousa, V.P., 2022. Lopinavir/ritonavir: a review of analytical methodologies for the drug substances, pharmaceutical formulations and biological matrices. Critic. Rev. Analyt. Chem. 52 (8), 1846–1862. https://doi.org/10.1080/10408347.2021.1920364.

Vithani, K., Goyanes, A., Jannin, V., Basit, A.W., Gaisford, S., Boyd, B.J., 2019. A proof of concept for 3D printing of solid lipid-based formulations of poorly water-soluble drugs to control formulation dispersion kinetics. Pharm. Res. 36 (7), 102. https://doi.org/10.1007/s11095-019-2639-y.

Vithani, K., Hawley, A., Jannin, V., Pouton, C., Boyd, B.J., 2017. Inclusion of digestible surfactants in solid SMEDDS formulation removes lag time and influences the formation of structured particles during digestion. AAPS J. 19 (3), 754–764. https://doi.org/10.1208/s12248-016-0036-6.

Williams, H.D., Speybroeck, M.V., Augustijns, P., Porter, C.J.H, 2014. Lipid-based formulations solidified via adsorption onto the mesoporous carrier neusilin® US2: effect of drug type and formulation composition on in vitro pharmaceutical performance. J. Pharm. Sci. 103 (6), 1734–1746. https://doi.org/10.1002/jps.23970.

Witzleb, R., Müllertz, A., Kanikanti, V.-R., Hamann, H.-J., Kleinebudde, P., 2012. Dissolution of solid lipid extrudates in biorelevant media. Int. J. Pharm. 422 (1–2), 116–124. https://doi.org/10.1016/j.ijpharm.2011.10.037.